

We are IntechOpen, the world's leading publisher of Open Access books Built by scientists, for scientists

6,900

Open access books available

186,000

International authors and editors

200M

Downloads

Our authors are among the

154

Countries delivered to

TOP 1%

most cited scientists

12.2%

Contributors from top 500 universities



WEB OF SCIENCE™

Selection of our books indexed in the Book Citation Index
in Web of Science™ Core Collection (BKCI)

Interested in publishing with us?
Contact book.department@intechopen.com

Numbers displayed above are based on latest data collected.
For more information visit www.intechopen.com



Nitrate Removal from Groundwater with Membrane Bioreactor

Marjana Simonič, Andreja Goršek and
Aleksandra Petrovič

Additional information is available at the end of the chapter

<http://dx.doi.org/10.5772/intechopen.68718>

Abstract

The aim of this study is to model the denitrification process performed in a membrane bioreactor (MBR). The research was carried out using a modified Zenon ZeeWeed 10 MBR system. The membrane module consisted of submerged hollow-fibre membrane with a pore size of $0.04\ \mu\text{m}$ and an active area of $0.93\ \text{m}^2$. The concentration of nitrate in drinking water was $(70 \pm 2)\ \text{mg/L NO}_3^-$. During the experiment, we maintained a constant concentration level of activated sludge at approximately $0.76\ \text{g/L}$ under anoxic conditions. Sugar was added to the activated sludge as a source of carbon. The Monod kinetic parameters were estimated based on the experimental data numerical interpolation. Afterwards, a dynamic simulation with known parameters was carried out, and the time dependence of the substrate and biomass concentration was studied. We developed a model based on actual substrate outlet concentration. In addition, the time required to reach a steady state was estimated.

Keywords: denitrification, groundwater, membrane bioreactor, dynamic concentration profile

1. Introduction

Nitrate and nitrite removal from water is necessary because of the harmful effects of nitrates on human health, such as methaemoglobinemia (blue-baby syndrome) [1–3], nitrosamines and nitrosamides [4].

During the biological process of denitrification, nitrate is microbiologically reduced over nitrite to molecular nitrogen (N_2) [1, 5]. The efficiency of biological removal of nitrate depends on different types of carbon sources [6, 7], various types of microorganisms [6, 8] and different

operational parameters such as carbon to nitrogen (C/N) ratios [2, 9], temperature [3, 10–12], pH [3, 10], dissolved oxygen [13, 14] and mixed liquor suspended solids (MLSSs) [15, 16]. Furthermore, it also depends on the amount of substrate and heterotrophic yield [17]. Denitrification may be inhibited by higher levels of nitrate and nitrite [10, 18, 19], which can directly affect microbial growth. Reaction rates and efficiencies are sensitive to dissolved oxygen [11]; anoxic growth reaction especially can be inhibited [17]. The advantages of heterotrophic denitrification are, on the one hand, the high denitrifying rates; on the other hand, one of the greater weaknesses is that the residual carbon sources can cause many problems during drinking water treatment [3]. For growth under anoxic conditions, heterotrophic denitrifiers require a specific source of organic carbon, such as methanol [1, 2, 6, 20], ethanol [2, 15, 21], acetate [7, 10], glucose [7, 9, 20], glycerol [20] and acetic acid [20], whilst the application of sucrose is relatively rare and has only been mentioned in a few articles [2]. Gómez et al. [2] studied the effectiveness of three selected carbon sources (sucrose, ethanol and methanol) on submerged filters for the removal of nitrate from contaminated groundwater (100 mg/L NO_3^-). Greater biomass production was observed with sucrose, compared with ethanol and methanol. Fernández-Nava et al. [4] examined the properties of saccharose-rich residue (from the production of soft drinks) in the process of denitrification. Crude syrup as a C source was used in another study performed by Lee and Welander [6]. Sison et al. [22] used sucrose in the process of denitrification by biological granular-activated carbon. The influent $\text{NO}_3\text{-N}$ concentration was 80 mg/L (C/N ratio 1.88:1), and the average denitrification efficiency achieved 84–89%. During the study, when the C/N ratio increased from 1.5 to 2.5, removal efficiency increased up to 95% [23]. Besides the influence of C sources, the investigations focused on different types of denitrification (hydrogenotrophic [19, 24], autotrophic [25], heterotrophic [25]), membrane bioreactor (MBR) configurations [16], carbon to nitrogen (C/N) ratio [15, 25–27], and the removal of pesticides [27]. Moreover, studies were carried out on hydraulic retention time [28–30], concentration of mixed liquor suspended solids (MLSSs) [15, 16, 30], mathematical modelling of MBR [31], optimisation of the energy demand [29], trihalomethane formation potential [11, 21, 28, 30] and the inhibition of nitrite [10, 19]. The first commercial-scale biological drinking water denitrification plant utilising hydrogen was introduced at Rassel in Germany [19, 24]. However, the MBR system is, in general, less commonly used for drinking water treatment. Nitrate removal from contaminated groundwater, drinking water and surface water has been studied by using extractive MBRs [31, 32], ion-exchange MBRs [16], gas-transfer MBRs [16], pressure-driven MBRs [15, 16, 28] and other known hybrid systems [11, 25]. The Zenon ZW 10 membrane bioreactor was first used in the denitrification of drinking water sources in 2005 [26].

Miscellaneous models for describing the process kinetics have been studied so far (e.g. the Haldane model and Michaelis-Menten kinetics). The performance of a special bacterial culture (*Aphelenchus avenae*) was investigated using different carbon sources, such as ethanol, methanol, sodium acetate, glucose and poly(ϵ -caprolactone), within the batch biological denitrification system [33]. The most commonly used relationship describing microbial growth is Monod kinetics [33–35]. This mechanism is also used to describe heterotrophic denitrification [19]. There are several factors affecting microbial growth and its kinetics: pH [10, 36], temperature [12, 36, 37], dissolved oxygen [11, 36], type of substrate [2, 9], microbial population [12, 37, 38], type of water

source [37] and the presence of nitrite [10]. The temperature dependence of the growth rate can generally be described using the Arrhenius relationship [39]. Microbial growth, Monod kinetics and the influences of different physico-chemical factors on the denitrification process have been extensively investigated in recent papers [34, 35, 39]. In an experiment by Ravindran et al. [11], mixed batch bioreactor studies were performed to evaluate the denitrification kinetics of groundwater. Ethanol was added as the external carbon source. A sensitivity analysis was performed in order to determine which biokinetic parameter had the greatest influence on effluent substrate concentration. The results obtained showed that biokinetic coefficients vary significantly with any changes in the MLSS concentrations of groundwater.

Studying biokinetic coefficients is important to obtain more information about the cell growth and utilisation of substrate, which then helps to better understand the denitrification process. A literature review shows that there is a lack of information related to the determination of kinetic coefficients for drinking water denitrification treatment by MBR using sugar as a C source.

The purpose of our research was to develop a kinetic model in order to describe microbial growth during the drinking water denitrification process using MBR. A kinetic study was conducted by assuming Monod kinetics to be appropriate for describing substrate consumption at constant biomass concentration. Firstly, the basic kinetic parameters, such as specific growth rate of biomass, substrate half-saturation constant and the yield coefficient, were determined based on experimental data. Furthermore, dynamic simulation was performed based on calculated kinetic parameters. With the dynamic concentration profiles, the time dependence of the substrate and biomass concentrations can be followed, and the time required to reach steady state can be estimated.

2. Materials and methods

During this study, denitrification was carried out in a modified Zenon ZW 10 MBR, which can be described as a continuous stirred-tank reactor (CSTR) with recycle capability. The microbial growth rate was expressed using Monod kinetics [34, 35, 39].

In our case, biomass was absent from the influent and effluent of the bioreactor, so the system behaved as a closed system (although the circulation of biomass within the reactor still existed). The fact that the increase of biomass was very low had to be taken into account during the calculations, in which the increase of biomass was neglected. Because of the biomass characteristics, it was assumed that the mode of MBR operation would be close to the model of mixed flow bioreactor under steady state. The substrate dynamic profiles could be described with the equations for the continuous stirred-tank reactor (CSTR) with recycle [40]. The mass balances for substrate and biomass [36, 40], provided a basis for determining a kinetic model regarding drinking water denitrification (Eqs. (1)–(26)). The balance of biomass was obtained in two ways: firstly, by using the equations for a continuous stirred-tank reactor with recycling, and secondly, by the equations for the reactor without recycling. During the testing of the second method, we assumed that the biomass concentration in the circulation is

equal to the concentration of biomass in the reactor and would thus produce the same result in both cases, namely that the specific growth rate of microorganisms is equal to the dilution rate.

2.1. Mass balance of biomass

Depending on the biomass and the mode of operation, the equations for the CSTR in steady state [36, 40] can be used (Eqs. (1)–(9)):

$$\text{Input} - \text{Output} + \text{Generation} = \text{Accumulation} \quad (1)$$

For each part of above Eq. (1), the following can be written:

$$q_D \gamma_D - q_X \gamma_X + \mu \gamma_X V = (d\gamma_X V/dt) \quad (2)$$

Eq. (2) can be written in the form:

$$q_D \gamma_D - q_X \gamma_X + \mu \gamma_X V = (d\gamma_X/dt)V + (dV/dt)\gamma_X \quad (3)$$

For the continuous stirred-tank reactor, $(dV/dt) = q_D - q_X = 0$, and from this it follows that $q_D = q_X = q$; therefore, it can be written and referred to as

$$q(\gamma_D - \gamma_X) + \mu \gamma_X V = (d\gamma_X/dt)V : V \quad (4)$$

And then

$$q/V(\gamma_D - \gamma_X) + \mu \gamma_X = d\gamma_X/dt \quad (5)$$

The *quotient* of the inlet flow rate and bioreactor volume can be expressed as, $D = q/V$ (h^{-1}). Dynamic changes in the biomass concentration over the time can be written as follows:

$$D(\gamma_D - \gamma_X) + \mu \gamma_X = d\gamma_X/dt \quad (6)$$

By considering that the inlet mass concentration of biomass is zero ($\gamma_D = 0$) and at steady state $d\gamma_X/dt = 0$, Eq. (6) can be expressed as

$$-D\gamma_X + \mu \gamma_X = 0 \quad (7)$$

And

$$D = \mu \quad (8)$$

Specific growth rate of biomass, μ , can be expressed as [35, 36]

$$\mu = \mu_{\text{Max}} \gamma_S / (K_S + \gamma_S) \quad (9)$$

At high substrate concentrations ($\gamma_S \gg K_S$), a zero-order kinetic model is usually used and at low-substrate concentrations, first-order dependence can be applied [10, 39].

The specific growth rate of active biomass is a result of the endogenous decay of active biomass (microbial death) reduced for the coefficient k_d (h^{-1}) [36]. Thus, Eq. (6) can be rearranged into Eq. (10):

$$D(\gamma_D - \gamma_X) + (\mu - k_d)\gamma_X = d\gamma_X/dt \quad (10)$$

And further:

$$d\gamma_X/dt = D(\gamma_D - \gamma_X) + (\mu_{\text{Max}}\gamma_S/(K_S + \gamma_S) - k_d)\gamma_X \quad (11)$$

Similarly, the mass balance of biomass for CSTR with recycling [36, 40], can be written according to Eqs. (12)–(20):

$$\text{Input} - \text{Output} + \text{Generation} = \text{Accumulation} \quad (12)$$

In steady state: Accumulation = 0

Similarly, Eq. (3), the next Eq. (13) can be written as

$$q_D\gamma_D + q_R\gamma_R - (q_D + q_R)\gamma_X + \mu\gamma_X V = 0 \quad (13)$$

Since $q_D\gamma_D = 0$ (biomass concentration at the inflow is zero), therefore

$$q_R\gamma_R - (q_D + q_R)\gamma_X + \mu\gamma_X V = 0 \quad (14)$$

If Eq. (14) is divided by V and afterwards by γ_X , then we obtain the following expression:

$$q_R\gamma_R/(V\gamma_X) - q_D/V - q_R/V + \mu = 0 \quad (15)$$

The dilution rate is the reciprocal value of residence time, $D = q_o/V$, therefore

$$\mu = D + q_R/V - q_R\gamma_R/(V\gamma_X) \quad (16)$$

With the introduction of parameter, $a = q_R/q_o$, we obtain Eq. (17):

$$\mu = D + aq_o/V - (aq_o\gamma_R/(V\gamma_X)) \quad (17)$$

And if the quotient γ_R/γ_X is replaced by parameter b , then Eq. (17) can be rewritten as

$$\mu = D + aD - aDb \quad (18)$$

Since in our bioreactor, there was no barrier (or cell separator) which could lead to changes in the concentrations, we assumed that the mass concentrations of biomass in the recycle and in the reactor are equal $\gamma_R = \gamma_X$. This leads to the assumption that $b = 1$ and from this it follows that the specific growth rate of the biomass is equal to the dilution rate, Eqs. (19) and (20).

$$\mu = D + aD - aD \quad (19)$$

And

$$\mu = D \quad (20)$$

In this way, the same final expression for biomass, as with the equations for the continuous stirred-tank reactor, was obtained.

2.2. Mass balance of substrate

Regarding the substrate, the equations for CSTR with recycle [36, 40], were adequate (Eqs. (21)–(26)):

$$\text{Input} - \text{Output} - \text{Consumption} = \text{Accumulation} \quad (21)$$

In steady state: Accumulation = 0

For the substrate according to Eq. (21), the following expression can be written:

$$q_D \gamma_{S,D} - q_D \gamma_S - (1/y_{X,S}) \mu \gamma_X V = 0 \quad (22)$$

If Eq. (22) is divided by V and by considering that $q_o/V = D$, we obtain:

$$D \gamma_{S,D} - D \gamma_S - (1/y_{X,S}) \mu \gamma_X = 0 \quad (23)$$

The yield coefficient can be determined according to Eq. (24), which describes the mass balance of substrate in the steady state.

$$D(\gamma_{S,D} - \gamma_S) = (1/\gamma_{X,S}) \mu \gamma_X \quad (24)$$

Since during the consumption of the substrate and thus in the production of biomass only active biomass is involved, the variable w_x is introduced into Eq. (24) representing the percentage of active biomass:

$$D(\gamma_{S,D} - \gamma_S) = (1/\gamma_{X,S}) \mu w_x \gamma_X \quad (25)$$

In the literature [8, 38, 41], information may be found about the proportion of active biomass, depending on a number of factors. The viability of biological sludge can be expressed as the active bacterial concentration per unit mass of volatile suspended solids [41].

Dynamic changes in the substrate concentration over time are displayed by the following Eq. (26):

$$D(\gamma_{S,D} - \gamma_S) - (1/\gamma_{X,S}) \mu_{\max} \gamma_X \gamma_S / (K_S + \gamma_S) = d\gamma_S/dt \quad (26)$$

2.3. Membrane bioreactor

Experiments were performed using the modified Zenon ZeeWeed 10 membrane bioreactor (MBR). The denitrification process was carried out under anoxic conditions in a reactor volume

of 60 L. The average operating temperature within the reactor was 26.3°C and the pH value within the range of (8.7–9.4). Variations in operating temperatures were a result of changes in the external temperatures. The membrane module consisted of a submerged hollow-fibre membrane with a pore size of 0.04 µm and a 0.93 m² active area. The process scheme for the drinking water treatment within the modified MBR is shown in **Figure 1** and the ultrafiltration (UF) membrane specifications are presented in **Table 1**.

The groundwater used for the study was spiked with sodium nitrate in concentration (70 ± 2) mg/L NO₃⁻. The membrane bioreactor (**Figure 2**) was inoculated with biomass sludge from an existing wastewater treatment plant. During the experiment, we maintained a constant

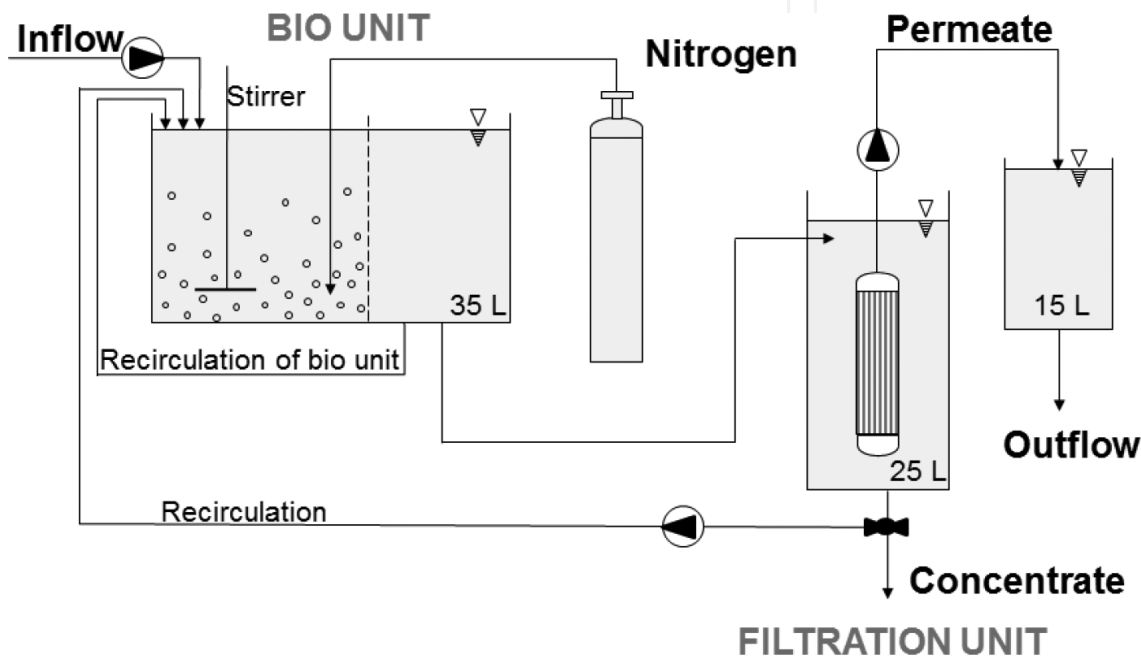


Figure 1. The process scheme for groundwater treatment with the modified MBR.

Specifications	Description
Type of membrane	Hollow fibre (HF)
Material	Polyvinylidene difluoride (PVDF)
Surface properties	Neutral, hydrophilic
Nominal membrane area	0.93 m ²
Pore size	0.04 µm
Max. temperature	40°C
pH range	5–9
Max. trans-membrane pressure	62 kPa
Max. pressure of backpulse	55 kPa
Max. capacity of process pumps	1.4 L/min

Table 1. UF membrane specifications.



Figure 2. Modified Zenon ZW 10 membrane module during the treatment.

concentration level of activated sludge at approximately 0.76 g/L. Anoxic conditions were provided by using nitrogen. Sugar was added to the activated sludge as a source of carbon. Inlet mass concentration of substrate was 0.1126 g/L. Based on previous papers [2, 22, 23] and our previous investigations, the appropriate value for the C/N ratio was 3:1.

A series of experiments were performed in order to follow the influence of drinking water flow rates (dilution rates) on the outlet's substrate concentration. The flow rate of the feed was increased stepwise, from 10 up to 170 mL/min. At each flow rate (or dilution rate), sufficient time was ensured to establish a steady state.

2.4. Analytical methods

Before, during, and after treatment of the drinking water, the following physico-chemical parameters were monitored: chemical oxygen demand (COD), content of nitrate ions NO_3^- and the mixed liquor suspended solids (MLSS). In addition, flow and circulation of water were monitored. Sugar concentration in the effluent was determined indirectly by measuring the chemical oxygen demand.

3. Results and discussion

Firstly, Monod kinetics parameters were determined.

During the experiment, we tried to maintain a constant concentration level of activated sludge within the reactor, 0.76 g/L expressed as MLSS and C/N ratio of 3:1. During the experiment, sugar concentration in the inflow was constant throughout all series. Such conditions allowed an average nitrate removal efficiency of 87%.

γ_s (mg/L)	D (h ⁻¹)
0	0
0.51	0.01
0.77	0.02
0.79	0.03
0.96	0.04
1.07	0.05
1.12	0.08
3.10	0.12
7.02	0.17

Table 2. Experimentally determined substrate mass concentration versus the dilution rate.

Determination of the kinetic parameters was based on the experimental values of outlet substrate mass concentration γ_s and the calculated dilution rates (D). The γ_s is expressed as chemical oxygen demand (COD). The data are gathered in **Table 2**.

Because of the low increment of biomass, changes in its concentration were negligible; therefore, MBR operation mode was close to that of a mixed flow bioreactor under steady state. For this reason, Eq. (8) could be adopted. The curve $D = f(\gamma_s)$ was plotted when compiling this equation, as shown in **Figure 3**. Subsequently, numerical interpolation using MATLAB software was performed.

The following results for Monod kinetics parameters were obtained: maximum specific growth rate of biomass, $\mu_{\max} = 0.31 \text{ h}^{-1}$ (7.4 d^{-1}) and the half-saturation constant (as COD) $K_s = 5.4 \text{ mg/L}$, both with $R^2 = 0.94$.

In the existing literature, there is a lack of information regarding the Monod parameters for drinking water denitrification, and it was impossible to find data relating the value of maximum specific growth rate and the half-saturation constant for systems similar to ours.

The yield coefficient was determined in the next step of our study and afterwards dynamic simulation was performed. The value of the yield coefficient was computed according to Eq. (25). This equation considered whether in the consumption of the substrate and thus during the production of biomass, only the active part of the biomass is involved. Sears et al. [8] reported that under typical operating conditions the microbial fraction of the activated sludge flocs represents approximately 40% by weight, whilst Chung and Neethling [41] reported that only 5–10% of the total volatile suspended solids represented active bacterial biomass. Similar values for MBR processes have been reported, namely that an active fraction of biomass [38] is between 4 and 7%. Based on these data, an active fraction of biomass (w_x) in our research was set at 5%. Numerical interpolation of experimental results (by the method of least squares) was performed in order to determine the yield coefficient ($Y_{X/S}$). The calculated value of the yield coefficient was ($Y_{X/S} = 0.35$ ($R^2 = 0.94$), which meant that approximately 35% of biomass was produced regarding the consumed substrate.

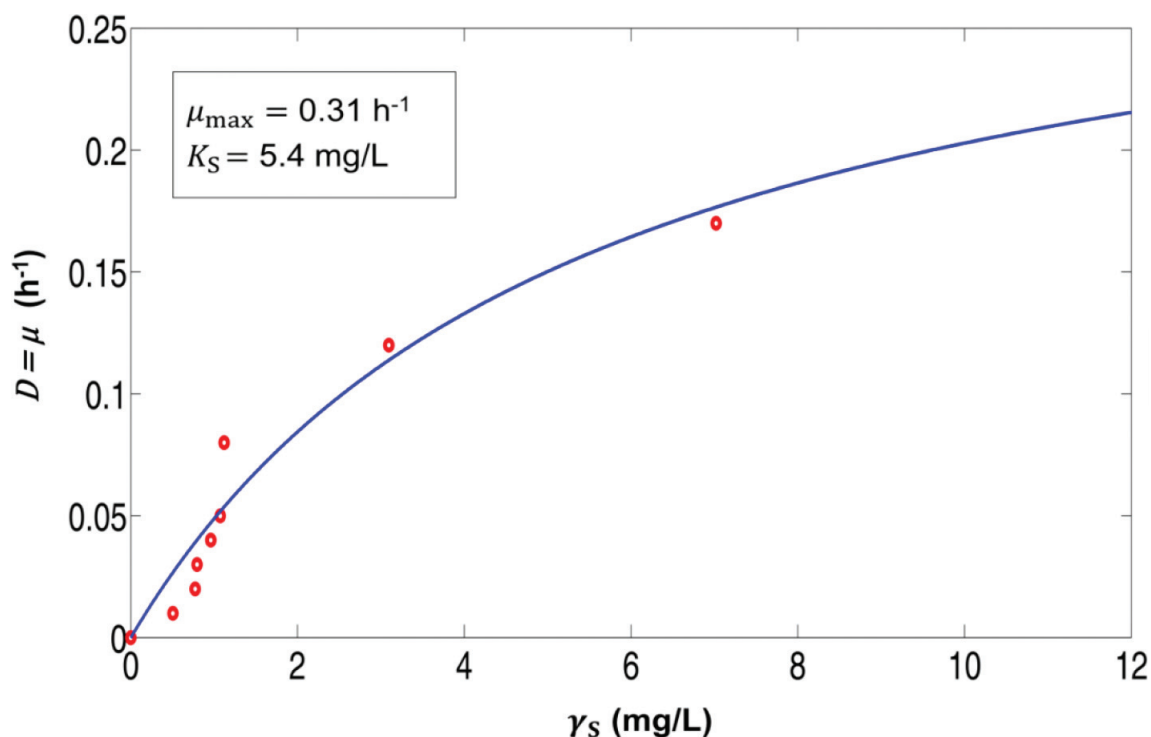


Figure 3. Specific growth rate of biomass as a function of substrate concentration at the outflow.

To date, no data for yield coefficient have been available for drinking water denitrification by MBR using sugar as the C source. The heterotrophic yield coefficient of activated sludge bacteria provides information about the biodegradability studies of chemical compounds and is important for modelling processes [42]. The removal of nitrate depends on the amount of substrate used and the heterotrophic yield [17]. In addition, product formation and yield coefficient are affected by temperature [36]. Lee and Welander [6], in their study on the effects of different carbon sources on respiratory denitrification, concluded that the carbon source had a significant influence on the denitrification rate, denitrification yield and the composition of the microflora. The growth yield for saccharose-rich crude syrup obtained during this study was within the range of 0.26–0.35 g TSS/g COD removed. The yield coefficient of aerobic organism growth using glucose was typically from 0.4 to 0.6, whilst the anaerobic growth was less efficient and the yield coefficient was reduced substantially [36].

3.1. Dynamic simulation

Dynamic simulation was performed based on the results obtained for μ_{\max} , K_S and $Y_{X/S}$. Using dynamic simulation by means of a software program, the time required to establish a steady state was estimated and the impact of the dilution rate on the concentration profiles of substrate and biomass was studied. The equations applied to this were: Eq. (11), which provides the dynamic changes of the biomass concentration over time, and Eq. (26), which describes the dynamic changes of the substrate concentration over time. The dilution rate varied from 0.1 up to 5 d^{-1} . The value for the specific endogenous decay rate for the heterotrophic biomass was determined at $k_d = 0.05 d^{-1}$. Dynamic simulation was performed according to the proposed

model by anticipating two different outlet substrate concentrations at the start of an operation (at the time of zero): first, the value of y_S close to zero (software allowed a minimal value 0.001 g/L) and second, the actual y_S is 0.1126 g/L. Dynamic concentration profiles are shown in **Figures 4** and **5**, respectively.

Figure 4 shows that by increasing the dilution rate, the time required to establish a steady state decreased. At lower flow rates, $D = 0.1 \text{ d}^{-1}$ (**Figure 4a**), the time needed to reach a steady state was over 25 days, but when the dilution rate increased ($D = 0.8$ and 1.2 d^{-1}), time decreased by up to 4–6 days, which can be seen in **Figure 4b** and **c**. At the higher flow rates (**Figure 4d**), however, this time can be shorter than 2.5 days. Whereas the microorganisms at the beginning of the operation needed to adapt to a new environment, the amount of biomass was low and the substrate concentration was high, and consequently less substrate was converted. After a while, the value of the substrate was reduced (because of increased consumption) and the biomass increased to a value corresponding to a steady state. The biomass concentration in the steady state increased when increasing the flow but only up to a certain limit. **Figure 4b** shows that a steady state was achieved after approximately 6 days of continuous operating. The

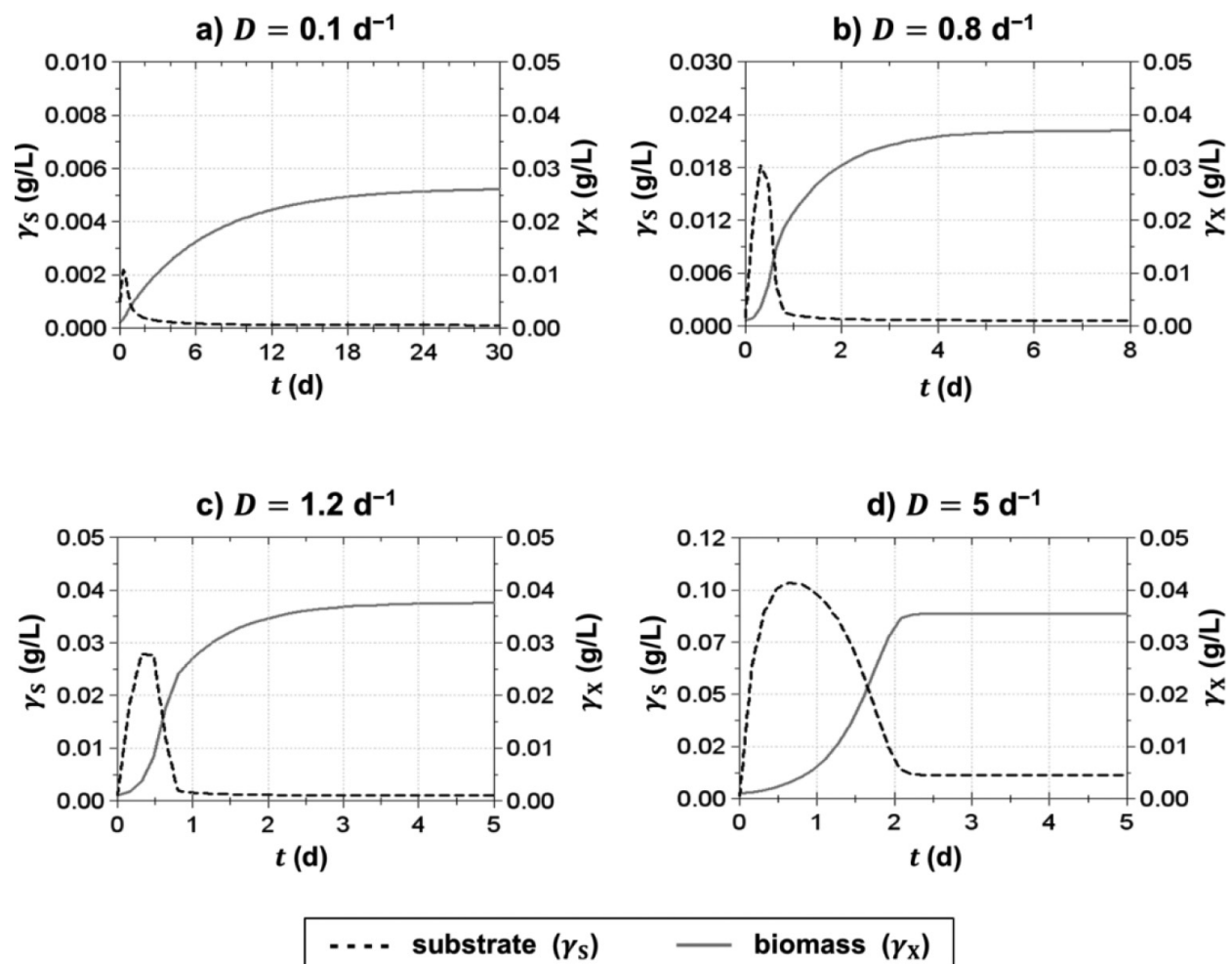


Figure 4. Dynamic concentration profiles for substrate ($\gamma_S = 0.001 \text{ g/L}$) and active biomass at four different dilution rates: (a) $D = 0.1 \text{ d}^{-1}$, (b) $D = 0.8 \text{ d}^{-1}$, (c) $D = 1.2 \text{ d}^{-1}$ and (d) $D = 5 \text{ d}^{-1}$.

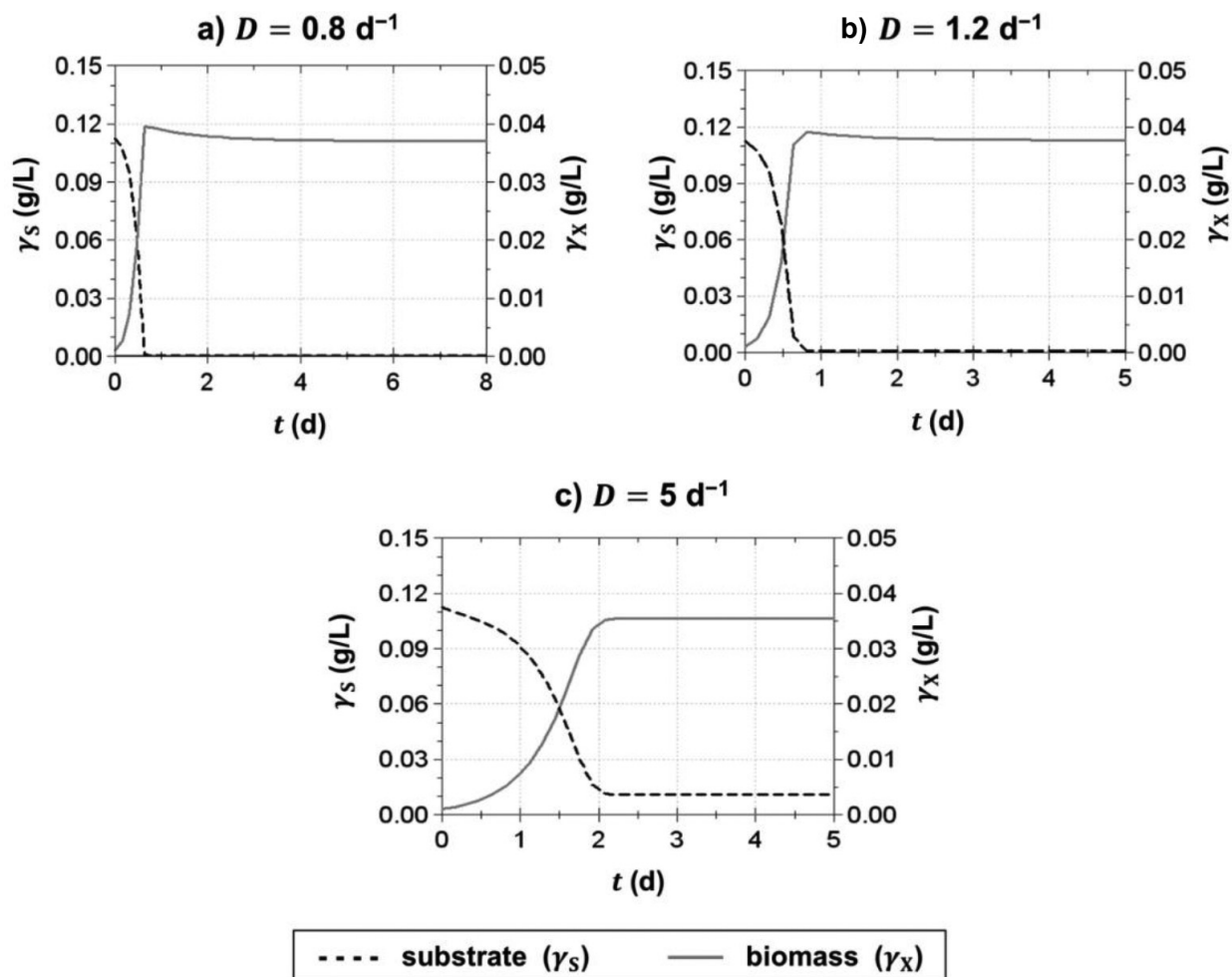


Figure 5. Dynamic concentration profiles ($\gamma_s = 0.1126 \text{ g/L}$) for substrate and active biomass at three different dilution rates: (a) $D = 0.8 \text{ d}^{-1}$, (b) $D = 1.2 \text{ d}^{-1}$ and (c) $D = 5 \text{ d}^{-1}$.

active biomass and substrate concentrations in the steady state were 37 and 0.8 mg/L, respectively. At a dilution rate of 1.2 d^{-1} (**Figure 4c**), a steady state was achieved in 4 days. The concentration of substrate in the steady state at this dilution rate increased to 1.5 mg/L, whilst the concentration of biomass was quite similar. At higher dilution rates, a steady state was achieved even faster, but the substrate concentration in the steady state increased up to 9 mg/L and the biomass concentration decreased up to 35 mg/L.

During the final phase of our research, we developed the second model based on actual outlet substrate concentration, 0.1126 g/L. By comparing **Figures 4** and **5**, it can be seen that the outlet substrate concentration at the start of an operation has an insignificant impact on the concentration of active biomass and substrate in the steady state. It caused a change in the shape of the profile only at the beginning of the operation. The times required to reach steady states (for each dilution rate) were practically the same as presented in **Figure 4**. **Figure 5a** shows that a steady state was achieved in approximately 5–6 days, which is almost the same as presented in **Figure 4b**. The same applied for dilution rate 5 d^{-1} , where the times needed to reach a steady state in both cases were shorter than 2.5 days (**Figures 4d** and **5c**). Therefore, it can be

concluded that outlet substrate concentration at the start of an operation has an insignificant impact on the final concentration of active biomass and substrate in the steady state.

4. Conclusion

Groundwater denitrification using a Zenon ZW 10 membrane bioreactor was studied and the validity verified regarding Monod kinetics for microbial growth. The research was carried out in two parts: firstly, the Monod kinetic parameters were determined by numerical interpolation of the experimental results and secondly, dynamic simulation was performed. The kinetic parameters obtained were 0.31 h^{-1} for the maximum specific growth rate of the biomass and 5.4 mg/L for the half-saturation constant. The calculated value of the yield coefficient was determined to be 35%. Using dynamic concentration profiles, the impact of the dilution rate on the substrate and biomass concentration was followed and the time required to establish a steady state was estimated. The results of dynamic simulation show that increase of the dilution rate decreased the time required to reach a steady state and that outlet substrate concentration has no significant impact on the concentration of the active biomass and substrate in the steady state.

Nomenclature

D	Dilution rate (h^{-1})
K_S	Half-saturation constant as COD (g/L)
q_D	Volume flow rate at the inflow (and at the outflow in the case of substrate mass balance) (L/h)
q_X	Volume flow rate at the outflow (L/h)
q_R	Volume flow rate at the recycle (L/h)
V	Reactor volume (L)
γ_D	Inflow mass concentration of biomass (g/L)
γ_X	Mass concentration of biomass in the reactor and at the outflow (g/L)
γ_R	Mass concentration of biomass at the recycle (g/L)
$\gamma_{S,D}$	Inflow mass concentration of substrate (g/L)
γ_S	Mass concentration of substrate at the outflow (g/L)
μ	Specific growth rate of biomass (h^{-1})
μ_{\max}	Maximum specific growth rate of biomass (h^{-1})
$Y_{X/S}$	Yield coefficient (biomass regarding substrate) (g/g)
w_X	Percentage of active biomass (%)
k_d	Endogenous decay rate (h^{-1})

COD	Chemical oxygen demand (mg/L)
TSS	Total suspended solids (g/L)
MLSS	Mixed liquor suspended solids (g/L)

Author details

Marjana Simonič*, Andreja Goršek and Aleksandra Petrovič

*Address all correspondence to: marjana.simonc@um.si

Faculty of Chemistry and Chemical Engineering, University of Maribor, Maribor, Slovenia

References

- [1] An S, Stone H, Nemati M. Biological removal of nitrate by an oil reservoir culture capable of autotrophic and heterotrophic activities: Kinetic evaluation and modeling of heterotrophic process. *Journal of Hazardous Materials*. 2011;**190**:686-693
- [2] Gómez MA, González-López J, Hontoria-García E. Influence of carbon source on nitrate removal of contaminated groundwater in a denitrifying submerged filter. *Journal of Hazardous Materials*. 2000;**80**:69-80
- [3] Karanasios KA, Vasiliadou IA, Pavlou S, Vayenas DV. Hydrogenotrophic denitrification of potable water: A review. *Journal of Hazardous Materials*. 2010;**180**:20-37
- [4] Fernández-Nava Y, Marañón E, Soons J, Castrillón L. Denitrification of high nitrate concentration wastewater using alternative carbon sources. *Journal of Hazardous Materials*. 2010;**173**:682-688
- [5] Wąsik E, Bohdziewicz J, Błaszczuk M. Removal of nitrates from groundwater by a hybrid process of biological denitrification and microfiltration membrane. *Process Biochemistry*. 2001;**37**:57-64
- [6] Lee NM, Welander T. The effect of different carbon sources on respiratory denitrification in biological wastewater treatment. *Journal of Fermentation and Bioengineering*. 1996;**82**:277-285
- [7] Shen J, He R, Han W, Sun X, Li J, Wang L. Biological denitrification of high-nitrate wastewater in a modified anoxic/oxic-membrane bioreactor (A/O-MBR). *Journal of Hazardous Materials*. 2009;**172**:595-600
- [8] Sears KJ, Alleman JE, Gong WL. Feasibility of using ultrasonic irradiation to recover active biomass from waste activated sludge. *Journal of Biotechnology*. 2005;**119**:389-399

- [9] Her J-J, Huang J-S. Influences of carbon source and C/N ratio on nitrate/nitrite denitrification and carbon breakthrough. *Bioresource Technology*. 1995;**54**:45-51
- [10] Glass C, Silverstein J. Denitrification kinetics of high nitrate concentration water: pH effect on inhibition and nitrite accumulation. *Water Research*. 1998;**32**:831-839
- [11] Ravindran V, Tsai H-H, Williams MD, Pirbazari M. Hybrid membrane bioreactor technology for small water treatment utilities: Process evaluation and primordial considerations. *Journal of Membrane Science*. 2009;**344**:39-54
- [12] Vacková L, Srb M, Stloukal R, Wanner J. Comparison of denitrification at low temperature using encapsulated *Paracoccus denitrificans*, *Pseudomonas fluorescens* and mixed culture. *Bioresource Technology*. 2011;**102**:4661-4666
- [13] Oh J, Silverstein J. Oxygen inhibition of activated sludge denitrification. *Water Research*. 1999;**33**:1925-1937
- [14] Sözen S, Çokgör EU, Orhon D, Henze M. Respirometric analysis of activated sludge behaviour—II. Heterotrophic growth under aerobic and anoxic conditions. *Water Research*. 1998;**32**:476-488
- [15] Nuhoglu A, Pekdemir T, Yildiz E, Keskinler B, Akay G. Drinking water denitrification by a membrane bio-reactor. *Water Research*. 2002;**36**:1155-1166
- [16] McAdam EJ, Judd SJ. A review of membrane bioreactor potential for nitrate removal from drinking water. *Desalination*. 2006;**196**:135-148
- [17] Fenu A, Guglielmi G, Jimenez J, Spèrandio M, Saroj D, Lesjean B, Brepols C, Thoeys C, Nopens I. Activated sludge model (ASM) based modelling of membrane bioreactor (MBR) processes: A critical review with special regard to MBR specificities. *Water Research*. 2010;**44**:4272-4294
- [18] Soto O, Aspé E, Roeckel M. Kinetics of cross-inhibited denitrification of a high load wastewater. *Enzyme and Microbial Technology*. 2007;**40**:1627-1634
- [19] Vasiliadou IA, Pavlou S, Vayenas DV. A kinetic study of hydrogenotrophic denitrification. *Process Biochemistry*. 2006;**41**:1401-1408
- [20] Akunna JC, Bizeau C, Moletta R. Nitrate and nitrite reductions with anaerobic sludge using various carbon sources: Glucose, glycerol, acetic acid, lactic acid and methanol. *Water Research*. 1993;**27**:1303-1312
- [21] McAdam EJ, Judd SJ. Denitrification from drinking water using a membrane bioreactor: Chemical and biochemical feasibility. *Water Research*. 2007;**41**:4242-4250
- [22] Sison NF, Hanaki K, Matsuo T. High loading denitrification by biological activated carbon process. *Water Research*. 1995;**29**:2776-2779
- [23] Sison NF, Hanaki K, Matsuo T. Denitrification with external carbon source utilizing adsorption and desorption capability of activated carbon. *Water Research*. 1996;**30**:217-227

- [24] Lee K-C, Rittmann BE. Applying a novel autohydrogenotrophic hollow-fiber membrane biofilm reactor for denitrification of drinking water. *Water Research*. 2002;**36**:2040-2052
- [25] Zhao Y, Zhang B, Feng C, Huang F, Zhang P, Zhang Z, Yang Y, Sugiura N. Behavior of autotrophic denitrification and heterotrophic denitrification in an intensified biofilm-electrode reactor for nitrate-contaminated drinking water treatment. *Bioresource Technology*. 2012;**107**:159-165
- [26] Buttiglieri G, Malpei F, Daverio E, Melchiori M, Nieman H, Ligthart J. Denitrification of drinking water sources by advanced biological treatment using a membrane bioreactor. *Desalination*. 2005;**178**:211-218
- [27] Aslan Ş. Combined removal of pesticides and nitrates in drinking waters using bionitrification and sand filter system. *Process Biochemistry*. 2005;**40**:417-424
- [28] Li X, Chu HP. Membrane bioreactor for the drinking water treatment of polluted surface water supplies. *Water Research*. 2003;**37**:4781-4791
- [29] McAdam E, Judd S. Optimisation of dead-end filtration conditions for an immersed anoxic membrane bioreactor. *Journal of Membrane Science*. 2008;**325**:940-946
- [30] Tian J, Liang H, Nan J, Yang Y, You S, Li G. Submerged membrane bioreactor (sMBR) for the treatment of contaminated raw water. *Chemical Engineering Journal*. 2009;**148**:296-305
- [31] Sanaeepur H, Hosseinkhani O, Kargari A, Ebadi Amooghin A, Raisi A. Mathematical modeling of a time-dependent extractive membrane bioreactor for denitrification of drinking water. *Desalination*. 2012;**289**:58-65
- [32] Ergas SJ, Rheinheimer DE. Drinking water denitrification using a membrane bioreactor. *Water Research*. 2004;**38**:3225-3232
- [33] Nalcaci OO, Böke N, Ovez B. Potential of the bacterial strain *Acidovorax avenae* subsp. *avenae* LMG 17238 and macro algae *Gracilaria verrucosa* for denitrification. *Desalination*. 2011;**274**:44-53
- [34] Al-Malack MH. Determination of biokinetic coefficients of an immersed membrane bioreactor. *Journal of Membrane Science*. 2006;**271**:47-58
- [35] Doran PM. *Bioprocess Engineering Principles*. Elsevier Science & Technology Books. 2004
- [36] Shuler ML, Kargi F. *Bioprocess Engineering, Basic Concepts*. 2nd ed. Prentice Hall . 2002
- [37] Peng J, Xue G. Mathematical modeling of hollow-fiber membrane system in biological wastewater treatment. *Journal of Systemics, Cybernetics and Informatics*. 2006;**4**:47-52
- [38] Di Trapani D, Capodici M, Cosenza A, Di Bella G, Mannina G, Torregrossa M, Viviani G. Evaluation of biomass activity and wastewater characterization in a UCT-MBR pilot plant by means of respirometric techniques. *Desalination*. 2011;**269**:190-197
- [39] Blanch WH, Clark SD. *Biochemical Engineering*. CRC press. 1997
- [40] Bailey JE, Ollis DF. *Biochemical Engineering Fundamentals*. 2nd ed. McGraw-Hill. 1986

- [41] Chung YC, Neethling JB. Viability of anaerobic digester sludge. *Journal of Environmental Engineering ASCE*. 1990;**116**:330-342
- [42] Strotmann UJ, Geldem A, Kuhn A, Gendig C, Klein S. Evaluation of a respirometric test method to determine the heterotrophic yield coefficient of activated sludge bacteria. *Chemosphere*. 1999;**38**:3555-3570

IntechOpen

IntechOpen

